Journal of Global Environment Engineering, Vol. 10, pp. 39-51, 2004

Full Paper

ESTIMATION OF THE EMISSION RATIO OF HYDROCARBONS FROM BIOMASS BURNING BY USING BACKWARD TRAJECTORY ANALYSIS FROM AIRBORNE OBSERVATION FOR EAST ASIA

Gakuji Kurata[1], *Toshihiro Kitada*[2], *Gregory R. Carmichael*[3]
Youhua Tang[4], *Jung-Hun Woo*[5]

Abstract

Emission ratios of CO and some NMHCs from various regions in East Asia, especially for the biomass burning in Southeast Asia, were estimated by using the backward trajectory analysis from NASA TRACE-P flight tracks and a numerical simulation with three-dimensional chemical transport model (STEM-2k1). These results were compared with bottom-up inventory and previous studies. The airmasses affected by the emission from biomass burning were easily distinguished by the ratio between a certain species and another one, and the source region of them was identified as Southeast Asia by trajectory analyses. Ratios of concentration among the observed species for the airmasses affected by biomass burning were corresponding with the suggested emission factors for the savanna and grassland. In addition, reconstructed field of the observed and modeled ratio among CO and NMHCs, such as ethane/CO and ethane/propane, by the backward trajectories agreed well with the emission ratios in East Asia. This kind of analysis may help to improve the emission factors from biomass burning and other anthropogenic combustion by observation-based inventory scheme.

KEYWORDS: *chemical transport model, trajectory analysis, emission inventory, biomass burning, tropospheric composition*

1. Introduction

Due to the rapid development of East Asia, the influence of the long-range transport of atmospheric pollutants to the northern Pacific, North America and Asia itself, is becoming serious. These pollutants alter the composition of tropospheric trace chemical species, and they affect a wide range of the phenomena from acid rain in East Asia to the global climate change (e.g. *Ramanathan et al,* 2001; *Phadnis et al*, 2000).

In addition to it, biomass burning is one of the important sources for global and regional tropospheric chemistry, especially for CO, hydrocarbons and some particulate matters, such as

1 Dr.Eng., Reseach Associate, Dep. of Ecological Eng. Toyohashi Univeristy of Technologoy, JAPAN
2 Dr.Eng., Professor, Dep. of Ecological Eng. Toyohashi Univeristy of Technologoy, JAPAN
3 Dr. Eng, Professor, Research Center for Global and Regional Research, The University of Iowa, Iowa, USA
4 Dr. Eng, Post doctoral fellow, Research Center for Global and Regional Research, The University of Iowa, Iowa, USA
5 Dr. Eng, Post doctoral fellow, Research Center for Global and Regional Research, The University of Iowa, Iowa, USA

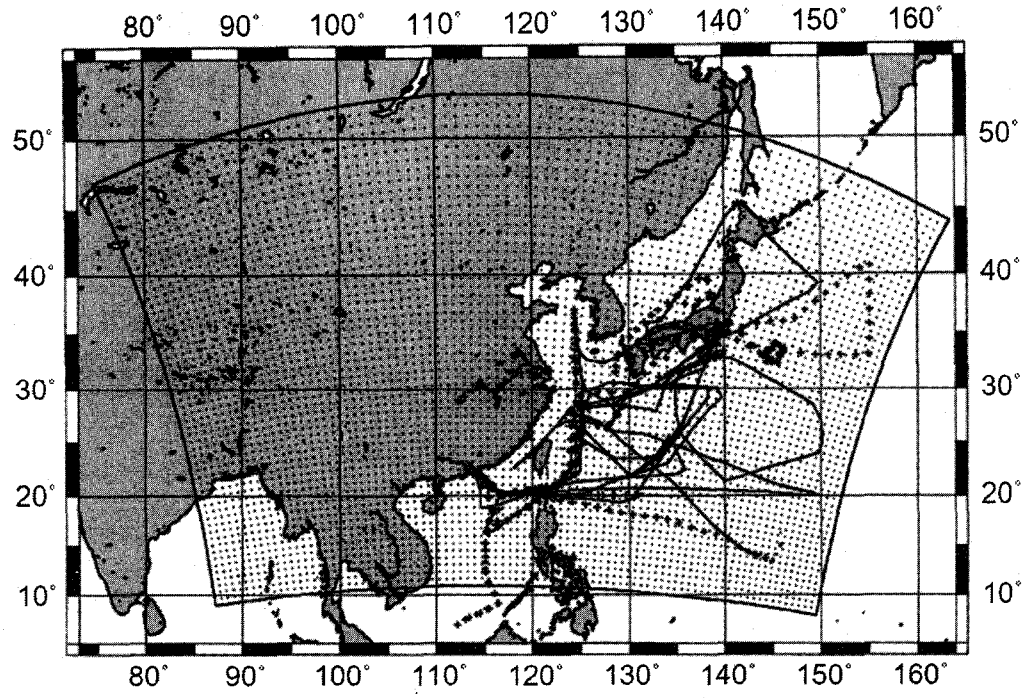

Fig.1 Flight tracks of each aircraft used in this analysis. Solid lines represent DC-8 and dashed lines represent P3B. Our analysis use DC8 #6 - #17 and P3B #8 - #19. Internal box and points represent model boundary and grid point.

black carbon and organic carbon. In the Indochinese Peninsula, February and March are the seasons when biomass burning is the most active. The total CO emission from biomass burning in whole East Asia for March 2001 was estimated to be 17.7 TgCO/month (*Woo et al.*, 2003). Most of these emissions were located in Southeast Asia. It is much higher than the total anthropogenic CO emission in Southeast Asia. Here, the estimation of the emission from biomass burning is based on the detection of the burning area from daily satellite images and the vegetation database. However, it is almost impossible to discriminate the condition of burning, which largely controls the emission factors of CO and hydrocarbons. Therefore, for the quantitative understanding of the contribution of the emission from biomass burning, further improvement of the estimation method and verification are still necessary.

TRACE-P was an aircraft observation campaign organized by NASA from February to April 2001. In this campaign, two aircraft, DC-8 and P-3B, observed a large number of gas-phase and aerosol species and meteorological and optical properties, with the goal to clarify the contribution of the anthropogenic pollution to the tropospheric chemical composition of the northern Pacific (*Jacob et al.*, 2003). Fig.1 shows the flight tracks of both aircraft over which the data were collected. Most of the observations were performed above the Yellow Sea, East China Sea, and South China Sea.

We applied a chemical transport model in forecast-mode to support the flight planning of

aircraft and the design of the observation strategies, and in post-analysis mode to interpret the observed data (*Carmichael, et al*, 2003a, 2003b). Emission inventories were developed to support this experiment (*Streets et al.*, and *Woo et al.*, 2003). However, large uncertainty, especially for emission of hydrocarbons, still exists due to the difficulty of the evaluation of the domestic biofuel consumption in the developing countries and biomass burning emission.

In this study, we developed the observation-based method to estimate emission distribution and intensities, and applied the method to the estimation of the emission ratios of the biomass burning. The observation-based scheme is based on the observation dataset and backward trajectories from the location of the observation. These techniques are very useful when the species are inert and time-independent. However, generally it is difficult to estimate accurate distribution of the source from this scheme, because there are many factors that affect the concentration of the species, such as transport, diffusion and mixing of the airmass, chemical reaction and deposition, etc. Therefore, we developed a hybrid method that combines both bottom-up and observation-based method, which can be used to improve the emission inventories.

2. Methodology

2.1. Chemical transport model

We use the STEM-2k1 chemical transport model (*Tang et al*, 2003) to simulate the distribution of trace species for this period. The chemical transport model was driven by the meteorological field calculated by meso-scale meteorological forecast system, CSU/RAMS, which used the ECMWF reanalysis data (6 hours interval, 1° x 1° horizontal resolution) for initial and boundary conditions (*Uno et al.*, 2003).

The chemical mechanism of STEM-2k1 is based on the SAPRC 99 (*Carter,* 2000), which consists of 93 species and 225 reactions. In addition, this version integrates on-line calculation of the photolysis rates, considering the influences of cloud, aerosol and gas-phase absorptions due to O_3, SO_2 and NO_2, using the NCAR Tropospheric Ultraviolet-Visible (TUV) radiation model. Boundary conditions were set to the lowest 5% at each altitude of the values observed during the TRACE-P operations in the western Pacific.

The emission datasets used in this calculation are based on *Streets et al.*, and *Woo et al.*, (2003). These are bottom-up inventories driven by regional-specific information on types of fuel and activity from various economic sectors (e.g., domestic, transport, power generation, industrial). These emission inventories include anthropogenic sources, biomass burning, volcanoes and biogenic source. Lightning NO_x, dust and sea salt emissions were estimated within the on-line CFORS framework (*Uno et. al.* 2003). The model domain is shown in Fig. 1. The horizontal coordinate of the model is in Lambert conformal projection and grid size is 80km, and the vertical domain was divided into 23 layers up to 23 km.

2.2. Backward trajectory analysis

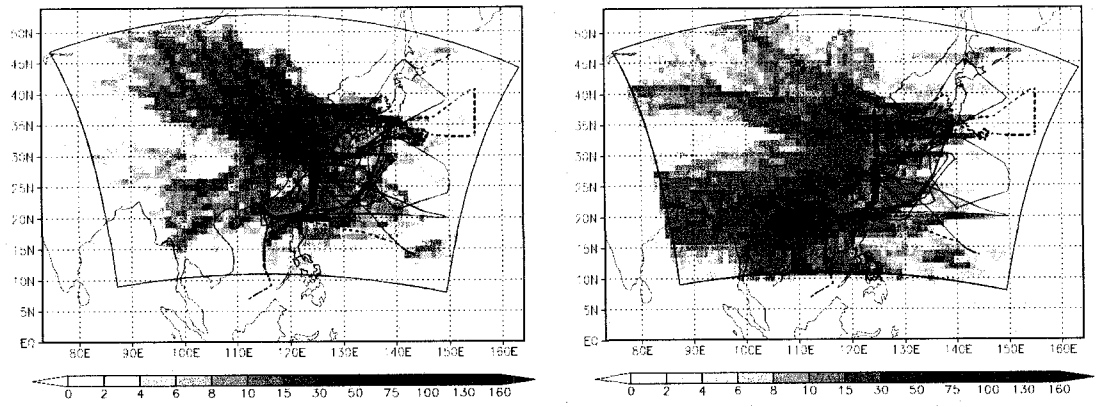

Fig. 2. The total number of the trajectories that passed over each mesh (1° x 1°) Altitude is defined as the height above land-surface.

In this study, we calculated 5-day backward trajectories from all 5-min segments of the flight tracks of both DC-8 and P-3B aircraft, using the three-dimensional RAMS meteorological fields. The kinematic method, which uses the vertical wind velocity from model output, was used for trajectory calculation. Total number of trajectories calculated was 2300. We also extracted the calculated concentration of each species, meteorological parameter, and photolysis rate along each trajectory from the three-dimensional model output. We used the observed data and extracted data from model output along the flight track and trajectories to reconstruct the horizontal and three-dimensional information, and compared them with the emission information.

3. Result

3.1. Backward trajectories

Fig.2 shows statistics associated with the number of the trajectories that passed over each mesh (1° x 1°) for all flights. Fig. 2 (a) and (b) show the number of the trajectories that passed under 3000m from the surface, and over 3000m, respectively. The airmasses that passed above 3000m were excluded from the following analysis, because those airmasses have a low possibility of being directly influenced by the surface emission. We see in the lower troposphere that airmasses tend to come from the northwest, while for heights over 3000m airmasses tend to come from the southwest. This feature means that the airmasses in the lower troposphere tend to be affected by the emission of the coastal industrial area of the northern China, and the airmasses in the middle troposphere tend to be affected by the emission of biomass burning at Southeast Asia.

The number of trajectories is very small from some region, such as northeastern part of India, Vietnam, and Cambodia. Some trajectories could not arrive to those areas in five days, because the general wind velocity is weak in low latitude. However, considering an accuracy of the

trajectories and deterioration of the airmasses, the calculation period was restricted to five days.

The grid cells with fewer than five trajectories were excluded from the following analysis. However many grid cells have a sufficient number of trajectories to estimate regional influences, including the biomass burning regions, such as northern Thailand and Myanmar.

3.2. Comparison of the concentration between model and observation

Fig. 3 shows the model performance for all points along the flight tracks, for CO, ethane, acetylene and propane, respectively. Each point represents the average of the observed values on the flight segment for every 5 minutes, and the average of the model results on the same flight leg. Most of the data points are within a factor two. In the case of CO and acetylene, any special biases are not seen between model and observation. However, In the case of ethane and propane, some underestimates are seen where the observed values are high concentration.

Fig. 4 shows the reconstructed concentration fields of CO, ethane, acetylene and propane, which were created by distributing the observed concentration to each mesh by using the backward trajectories.

The reconstructed concentration on each mesh is defined by following equation.

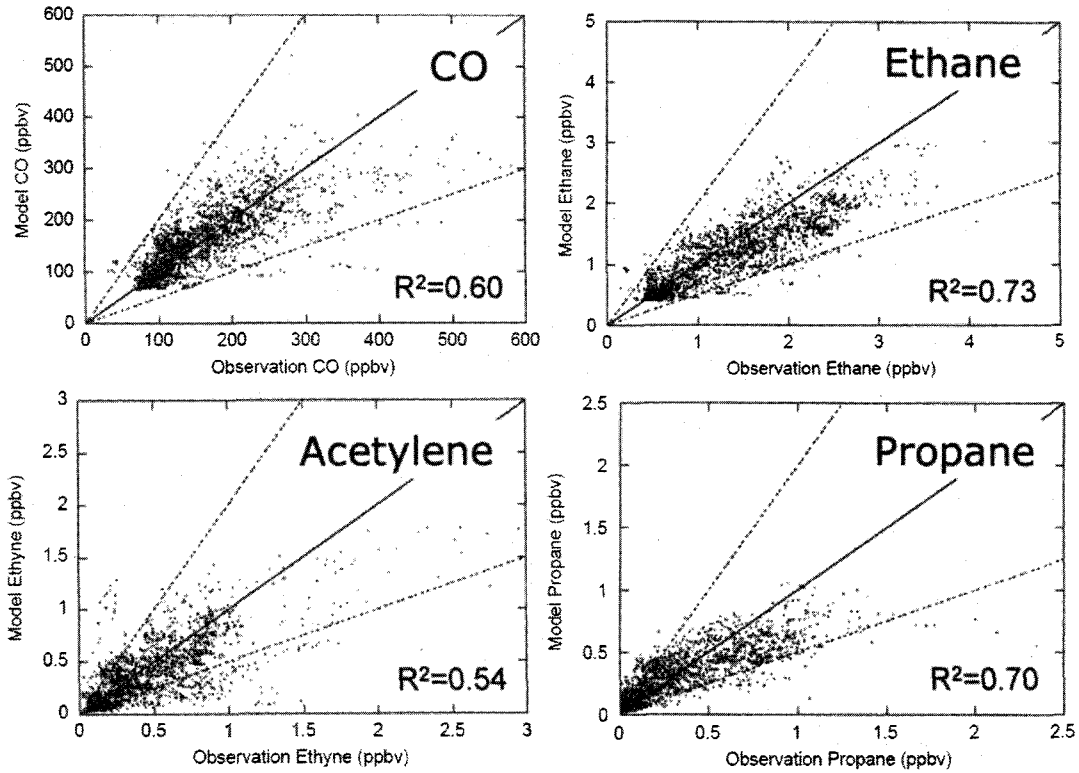

Fig. 3. Comparison of measured and modeled value on the flight tracks every 5-minute for both aircrafts. Broken lines represent factor 2. R^2 is a coefficient of the determination for linear regression.

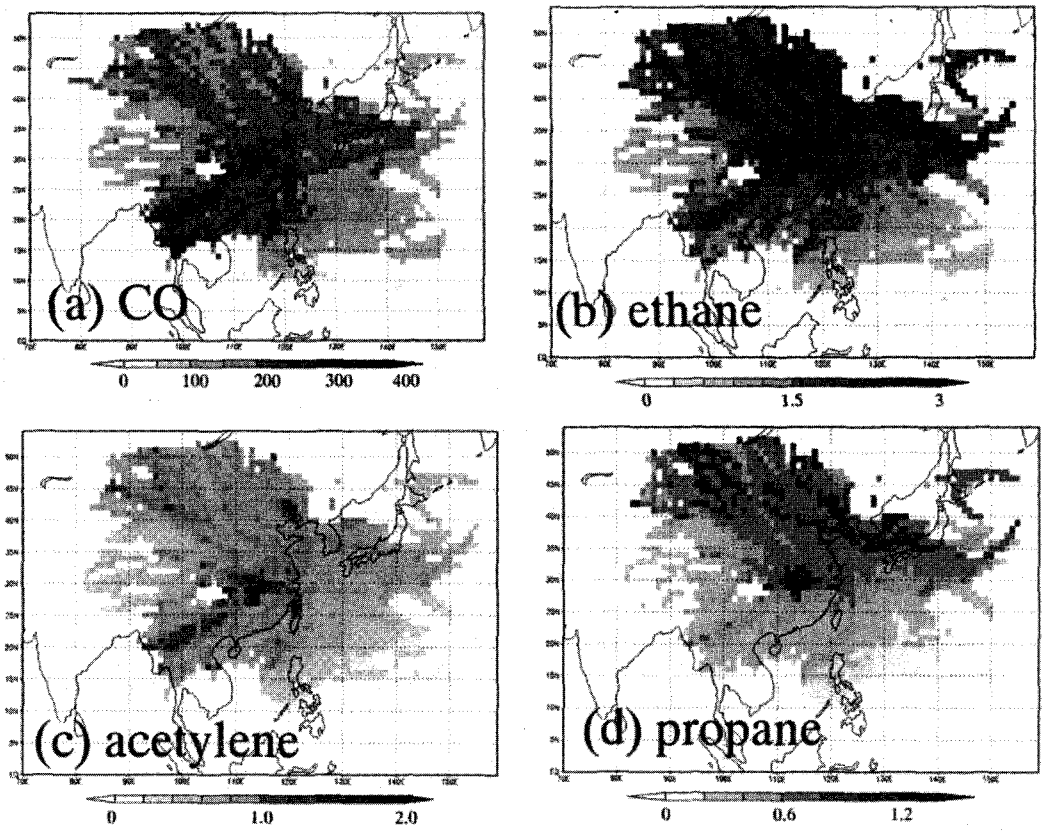

Fig. 4. Reconstructed concentration field which was created by distributing the observed concentration to each mesh by using the backward trajectories. (a) CO (b) Ethane (c) Acetylene (d) Propane (ppbv). All trajectories passed within 3000m of surface of each mesh were used.

$$C = \frac{1}{N}\sum_{i}^{N} C_i \tag{1}$$

Here, N is the number of the trajectories that passed over each mesh under 3000m above the ground. C_i denotes the observed concentration on the airplane that is associated with the specified back trajectory. Please note that the averaged concentration, C, does not include any atmospheric processing, such as chemical reaction, deposition and mixing, during transport from the location above mesh to the observed location. Moreover, the emission that the airmass received from other than the target mesh is treated as a noise. Therefore, this method has the limitations that the signal of the mesh with small emission is masked by those noises, and cannot be reproduced appropriately.

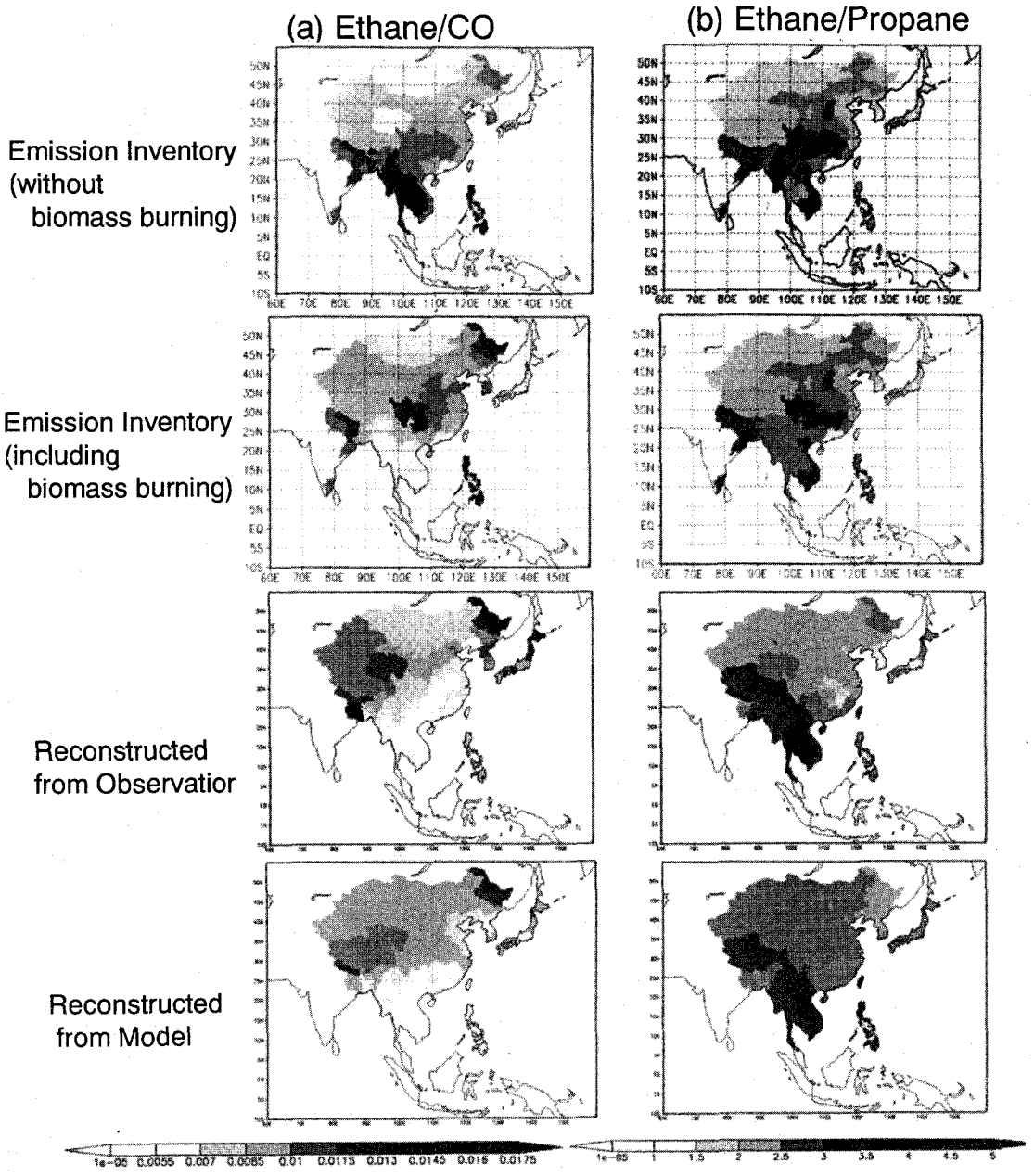

Fig.5 Emission ratio (with and without biomass burning emission) and reconstructed ratio from observation and model calculation by using backward trajectories. Reconstructed ratios from observation and model calculation are regression slope after subtracting background concentration, which was derived as a function of potential temperature. All trajectories passed within 3000m of surface of each mesh were used.

Fig. 4 (a) shows the average of observed CO calculated in this way. Very high average CO concentrations (>350ppbv) were seen for airmasses that passed over inland area of China area and Southeast Asia. CO emissions in inland area of China are very large from both industry and domestic use of biofuel and fossil fuel. During this period, biomass burning in Southeast Asia was also a major source of CO. On the other hand, the relatively small average CO levels (100-150ppbv) were associated with airmasses from the Pacific Ocean.

Fig. 4 (b) - (d) present the results for ethane, acetylene and propane, respectively. For the ethane and propane, there are large gradients from north to south. In the case of acetylene, we see high concentrations in the same areas as CO, but there is no significant north-south gradient.

3.3. Comparison of the ratio between model and observation

The ratios among the species are used in this section instead of the concentrations. Some of these ratios, such as acetylene/CO, have been suggested to be an indicator of atmospheric processing (*Smyth et al.*, 1996) (*McKeen et al.*, 1996), and the range of variability of their values in emission factors is very wide. Therefore, the combinations of these ratios will be useful to classify the airmasses in terms of atmospheric processing and the relationship with emission source.

The top panel of the Fig. 5 (a) is an emission ratio of ethane to CO, derived from the emission inventory without biomass burning emission. Second panel is same as top one, but an estimated emission from biomass burning during the campaign period, March 5 – 15, 2001, is taken into account. Daily emission of biomass burning was estimated from daily satellite image and vegetation database. Third and the bottom panels are the reconstructed ratios from observations and model calculation at the flight tracks, respectively, by using backward trajectories. These ratios were defined as a regression slope between the same combinations of species. Since CO and ethane have considerable background concentration, we first subtracted the background concentration. Background concentrations were determined as a function of potential temperature. Fig.6 shows these relationships between the observed concentrations and

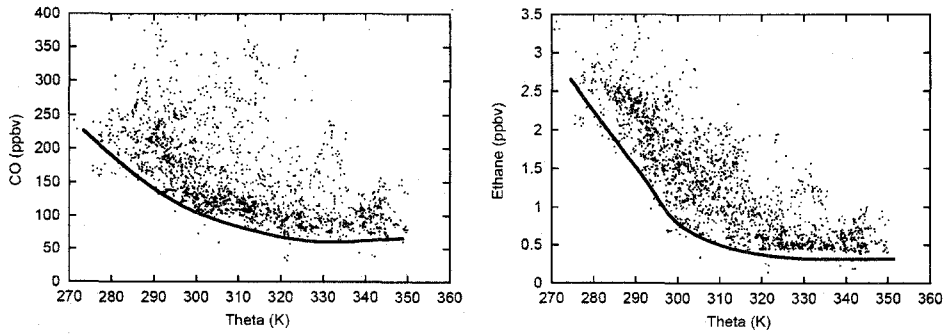

Fig.6 Scatter plot between the concentration and potential temperature (Theta).
(A) CO vs. Potential Temperature (B) Ethane vs. Potential Temperature. Baselines of these relationships are used as background concentration in this study.

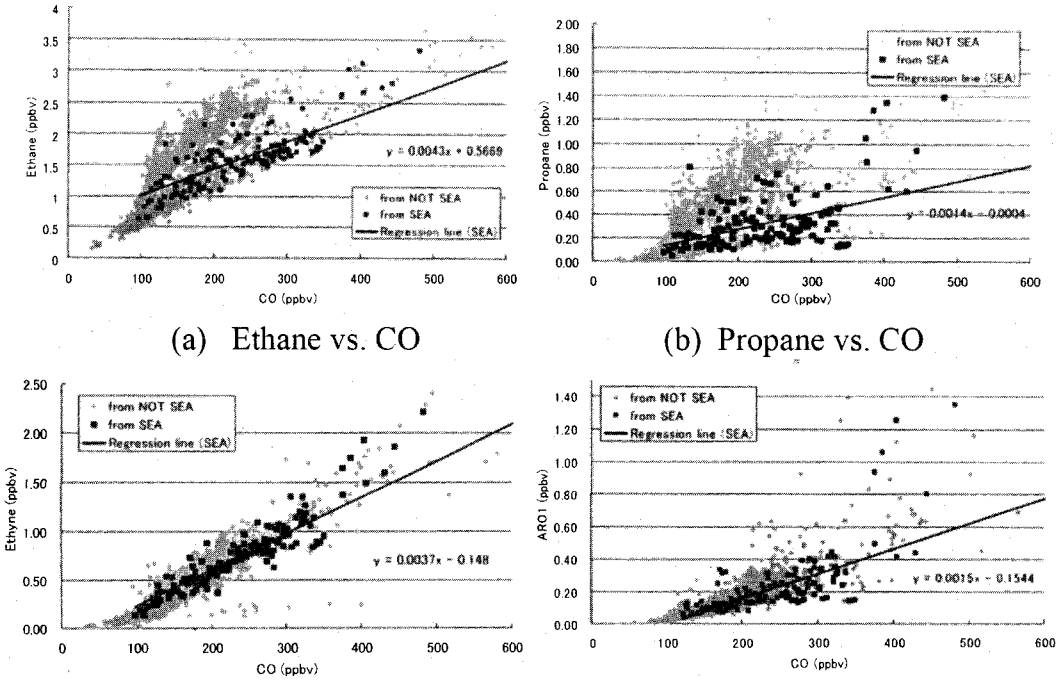

(a) Ethane vs. CO (b) Propane vs. CO

(c) Acetylene vs. CO (d) Benzen vs. CO

Fig. 7 Scatter plots on some hydrocarbons vs. CO for Observation data (a) Propane/CO (b) Ethyne/CO (c) Acetylene/CO (d) Benzene vs. CO, Black points represent the value for the airmass come from Southeast Asia (SEA). Grey points represent airmass from other region.

potential temperature. The baseline of Fig.6 (A) and (B) were assumed as a background concentration in this study.

In the case of an ethane/CO ratio, the reconstructed ratios from observation and model calculation are roughly similar in terms of both spatial pattern and value range. The range of these ratios at southern China and Southeast Asia (SEA) is about 0.005 or less. It is also consistent with the range of emission ratio including biomass burning emission.

In the case of the emission ratio that does not include biomass burning, the ethane/CO ratio on SEA region is large (from 0.013 to 0.018), and differs from the ratio of the observed airmasses distinctly.

Fig. 5 (b) shows the ratio of ethane/propane. In this case, the value range of the reconstructed ratios from the observations at SEA region is similar to that of emission ratios including biomass burning emission. The ratio from model calculation also shows the same qualitative features.

3.4. Estimation of the emission ratio from biomass burning in Southeast Asia

Fig. 7 are the scatter plots of the observed data on ethane vs. CO, propane vs. CO, acetylene vs. CO and benzene vs. CO, respectively. Black points represent the values for the airmasses that

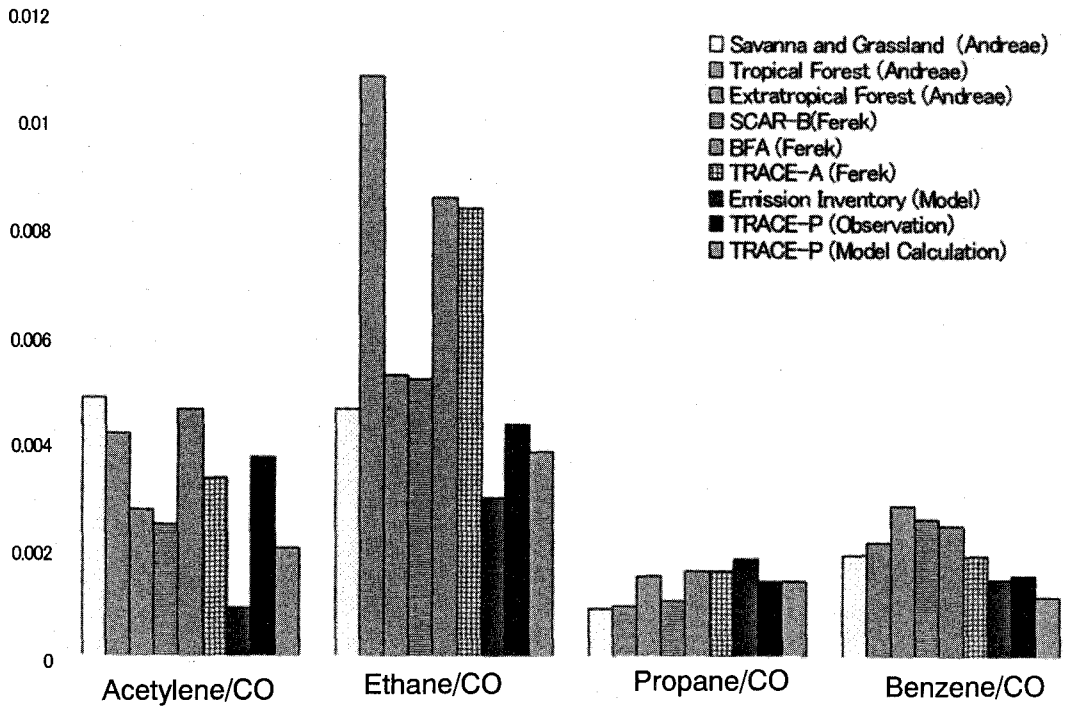

Fig. 8: Emission ratio of the biomass burning for acetylene, ethane, propane and benzene against CO from previous works and calculated value for both observation and model calculation in this work. [ppbv/ppbv]

passed over SEA region and grey points represent airmasses from other region. Solid line represents the regression line for SEA airmass. In the case of ethane vs. CO and propane vs. CO, regression slope for the airmasses from SEA was completely different from the airmasses from other region. The regression slope of ethane/CO for the observed airmasses from SEA is 0.0043. The emission ratio of ethane/CO for Thailand, when not including the emission from biomass burning, is 0.02, and for Myanmar is 0.013 (*Streets, et al.,* 2003). On the other hand, emission ratio of ethane/CO from burning of savanna and grassland is about 0.005 (*Andreae et al.*, 2001). Since the observed ratios were close to the ratio of biomass burning, it can be said that the airmasses that have passed through the lower troposphere at Southeast Asia during TRACE-P period had mainly received the influence of emission from biomass burning.

In the case of acetylene vs. CO, there is no significant difference between the airmasses from SEA and other region. Both species are associated with the incomplete combustion, and their correlation is very high. This means that the acetylene can be used as the alternative reference species of the combustion. There is an advantage that the background concentrations of acetylene do not have large latitudinal variation than that of CO.

Next, the regression slope of hydrocarbons against CO was compared with the emission ratio of various previous researches for the biomass burning emission and the emission ratio that we used in the model calculation. Fig. 8 include various emission ratio estimated in previous papers. (*Andreae et. al*, 2001 and *Ferek et. al,* 1998). Observed ratio for acetylene/CO during TRACE-P

(= 0.0037) was close to the emission ratio of the biomass burning from tropical forest (0.0048) or savanna (0.0041). Emission ratio used in the model calculation (= 0.0009) was much smaller than these values. In the case of ethane/CO, observed ratio (= 0.0043) was close to the ratio from savanna and grassland (0.0046) rather than tropical forest (0.010). Emission ratio used in the model calculation (0.0029) was also smaller than these values.

In the case of propane/CO, observed ratio (= 0.0014) was slightly larger than the emission ratio for savanna and grassland (= 0.00088). The emission ratio of propane/CO used in the model calculation was slightly larger than the observed ratio and previous works. On the other hand, observed ratio for benzene/CO (= 0.0015) was slightly smaller than the emission ratio (= 0.0018).

In Fig. 8, there is a clear difference between the ratio determined by the model calculation using same method as for the observation case and the emission inventory used in the model calculation. In the case of acetylene/CO, the ratio from model calculation is twice the emission ratio. This means that the ratio changes due to the chemical reaction or mixture during long-range transport. To estimate an exact emission ratio for such a combination of species from observation data, the consideration of chemical reaction, deposition and mixture during the transport will be necessary. Chemical transport model can provide such information.

4. SUMMARY

The model capability for associating the observed airmass with source regions was investigated, using chemical transport model, STEM-2k1, and backward trajectory analysis framework. The chemical transport model well reproduced the spatial and temporal distributions of CO and other NMHCs along the flight tracks.

Backward trajectory analysis coupled with the observed concentration and ratios between CO, ethane, propane and acetylene were compared with emission inventories and their ratios. From the reconstructed concentration field from observed CO concentration, high CO concentration was found at central China and Southeast Asia, where the heavy industry or biomass burning were very active. In addition, observed ethane/propane ratio was roughly agreed with that of emission ratios, which include the biomass burning emissions during observation period, in a spatial and temporal viewpoint.

Then, the analysis for estimating the emission ratios from biomass burning was carried out. We first estimated the emission ratio from biomass burning by using the regression slope from observed data that classified as the airmasses from Southeast Asia. Comparison with the ratio in the previous paper (Andreae et al., 2000) and the emission ratio used in our model calculation suggest that the emission ratio of acetylene/CO and ethane/CO was underestimate and propane/CO was slightly overestimate. The reconstructed ratios from observed data were well in agreement with the emission ratios for savanna and grassland in the Andrea's report.

From these analyses coupled with backward trajectory, we could find much important information associated with emission inventories. However, to make the systematic scheme to improve the emission estimate coupled with this kind of analysis, further detail consideration is necessary.

Acknowledgement

Part of this work was supported by the 21st Century COE Program "Ecological Engineering for Homeostatic Human Activities", from the Ministry of Education, Culture, Sports, Science and Technology of Japan.

Reference

Andreae, M. O. and Merlet, P. (2001): Emission of trace gases and aerosols from biomass burning, Global Biogeochemical Cycles, 15, 955-966.

Carmichael, G. R., Tang, Y., Kurata, G., Uno, I., Streets, D.G., Woo, J.-H., Huang, H., Yienger, J., Lefer, B., Shetter, R.E., Blake, D.R., Atlas, E., Fried, A., Apel, E., Eisele, F., Cantrell, C., Avery, M.A., Barrick, J.D., Sachse, G.W., Brune, W.L., Sandholm, S.T., Kondo, Y., Singh, H.B., Talbot, R.W., Bandy, A., Thorton, D., Clarke, A.D. and Heikes, B.G. (2003a): Regional-Scale Chemical Transport Modeling in Support of the analysis of observations obtained during the TRACE-P experiment, Journal of Geophysical Research, 108(D21), 8823, doi:10.1029/2002JD003117.

Carmichael, G. R., Tang, Y., Kurata, G., Uno, I., Streets, D.G., Thongboonchoo, N., Woo, J.-H., Guttikundi, S., White, A., Wang, T., Blake, D.R., Atlas, E., Fried, A., Potter, B., Avery, M.A., Sachse, G.W., Sandholm, S.T., Kondo, Y., Talbot, R.W., Bandy, A., Thorton, D. and Clarke, A.D. (2003b): Evaluating Regional Emission Estimates Using The TRACE-P Observations , Journal of Geophysical Research, 108(D21), 8810, doi:10.1029/2002JD003116.

Carter, W. (2000): Documentation of the SAPRC-99 chemical mechanism for VOC reactivity assessment, Final report to California Air Resources Board Contract No. 92-329, University of California Riverside.

Ferek, R. J., Reid, J. S., Hobbs, P. V., Blake, D. R. and Liousse, C. (1998): Emission factors of hydrocarbons, halocarbons, trace gases and particles from biomass burning in Brazil, Journal of Geophysical Research, Vol.103, pp.32,107-32,118.

Jacob, D. J., Crawford, J. H., Kleb, M. M., Connors, V. S., Bendura, R. J., Raper, J. L., Sachse, G. W., Gille, J. C., Emmons, L. and Heald, C. L. (2003): Transport and Chemical Evolution over the Pacific (TRACE-P) aircraft mission: Design, execution, and first results, Journal of Geophysical Research, 108 (D20), doi:10.1029/2002JD003276.

McKeen, S. A., Liu, S. C., Hsie, E.-Y., Liu, X., Bradshaw, J., Smyth, S. D., Gregory, G. L. and Blake, D. R. (1996): Hydrocarbon ratios during PEM-WEST A: A model perspective, Journal of Geophysical Research, Vol.101, 2087-2109.

Phadnis, M. J. and Carmichael, G. R. (2000): Transport and distribution of primary and secondary nonmethane volatile organic compounds in east Asia under continental outflow conditions, Journal of Geophysical Research, Vol.105, pp.22,311-22,336.

Ramanathan, V., Crutzen, P. J., Kiehl, J. T. and Rosenfeld, D. (2001): Aerosols, Climate, and the Hydrological Cycle, Science, 294, 2119-2124.

Smyth, S., Bradshaw, J., Sandholm, S., Liu, S., McKeen, S., Gregory, G., Anderson, B., Talbot, R., Blake, D., Rowland, S., Browell, E., Fenn, M., Merrill, J., Bachmeier, S., Sachse, G., Collins, J.,

Thornton, D., Davis and D., Singh, H. (1996): Comparison of free tropospheric western Pacific air mass classification schemes for the PEM-West A experiment, Journal of Geophysical Research, Vol.101, pp.1743-1762.

Street, D. G., Bond, T. C., Carmichael, G. R., Fernandes, S. D., Fu, Q., He, D., Klimont, Z., Nelson, S. M., Tsai, N. Y., Wang, M. Q., Woo, J.-H. and Yarber, K. F. (2003): An inventory of gaseous and primary aerosol emissions in Asia in the year 2000, J. Geophysical Research, 108 (D21),8809 , doi:10.1029/2002JD003093.

Tang, Y., Carmichael, G. R., Uno I., Woo, J.-H., Kurata, G., Lefer, B., Shetter, R. E., Huang, H., Anderson, B. E., Avery, M. A., Clarke, T. D. and Blake, D. R. (2003): Impacts of Aerosols and Clouds on Photolysis Frequencies and Photochemistry During TRACE-P: 2. Three-Dimensional Study Using a Regional Chemical Transport Model, Journal of Geophysical Research, 108 (D21) , 8822, doi:10.1029/2002JD003100.

Uno, I., Carmichael, G. R., Streets, D. G., Tang, Y., Yienger, J. J., Satake, S., Wang, Z., Woo, J.-H., Guttikunda, S., Uematsu M., Matsumoto K., Tanimoto H., Yoshioka K. and Iida, T. (2003): Regional chemical weather forecasting system CFORS: Model descriptions and analysis of surface observations at Japanese island stations during the ACE-Asia experiment, J. Geophys. Res., 108(D23), 8668, doi:10.1029/2002JD002845.

Woo, J.-H., Streets, D., Carmichael, G. R., Tang, Y., Yoo, B., Lee, W.-C., Thongboonchoo, N., Pinnock, S., Kurata G., Uno I., Fu, Q., Vay, S., Sachse, G. W., Blake, D. R., Fried, A. and Thornton, D. C., (2003): The contribution of biomass and biofuel emissions to trace gas distributions in Asia during the TRACE-P Experiment, J. Geophysical Research, 108 (D21), 8812, doi:10.1029/2002JD003200.